

Scheemaeker Stephanie (Orcid ID: 0000-0003-1480-5056)

**Organoids of patient-derived medullary thyroid carcinoma: the first milestone towards a new *in vitro* model in dogs**

**Organoids of patient-derived medullary thyroid carcinoma: the first milestone towards a new *in vitro* model in dogs**

Stephanie Scheemaeker<sup>1</sup>, Marine Inglebert<sup>2</sup>, Sylvie Daminet<sup>1</sup>, Martina Dettwiler<sup>2</sup>, Anna Letko<sup>3</sup>, Cord Drögemüller<sup>3</sup>, Martin Kessler<sup>4</sup>, Richard Ducatelle<sup>5</sup>, Sven Rottenberg<sup>2</sup>, Miguel Campos<sup>6</sup>

<sup>1</sup> Department of Small Animals, Faculty of Veterinary Medicine, Ghent University, Salisburylaan 133, 9820 Merelbeke, Belgium

<sup>2</sup> Department of Infectious Diseases and Pathobiology, Vetsuisse Faculty, University of Bern, Länggassstrasse 122, 3012 Bern, Switzerland

<sup>3</sup> Institute of Genetics, Vetsuisse Faculty, University of Bern, Bremgartenstrasse 109a, 3012 Bern, Switzerland

<sup>4</sup> Tierklinik Hofheim, Katharina-Kemmler-Straße 7, 65719 Hofheim am Taunus, Germany

<sup>5</sup> Department of Pathobiology, Pharmacology and Zoological Medicine, Faculty of Veterinary Medicine, Ghent University, Salisburylaan 133, 9820 Merelbeke, Belgium

<sup>6</sup> Department of Clinical Veterinary Science, Vetsuisse Faculty, University of Bern, Länggassstrasse 128, 3012 Bern, Switzerland

This article has been accepted for publication and undergone full peer review but has not been through the copyediting, typesetting, pagination and proofreading process which may lead to differences between this version and the [Version of Record](https://doi.org/10.1111/vco.12872). Please cite this article as doi: [10.1111/vco.12872](https://doi.org/10.1111/vco.12872)

This article is protected by copyright. All rights reserved.

Accepted Article

### **Acknowledgements**

We want to thank Sarah Loomans (Department of Pathobiology, Pharmacology and Zoological Medicine, Ghent University) for performing the immunohistochemical stainings for COX-2, P-glycoprotein and VEGF. Also, a special thanks to Dr. Sara Soto (Department of Infectious Diseases and Pathobiology, University of Bern) for her support in planning the synaptophysin immunolabeling at Pathologie Länggasse (Ittigen, Switzerland). We are also thankful to Ghent University, the Research Foundation - Flanders (FWO) and the ESVE for their financial support.

Results were presented as an oral abstract at the online 31<sup>st</sup> ECVIM-CA 2021 congress. The oral abstract received the first oral abstract price, the ESVE-MSD Animal Health award, at the 31<sup>st</sup> ECVIM-CA 2021 congress and was, therefore, also presented at the hybrid ACVIM Forum 2022.

### **Funding information**

This research was funded by the ESVE biobank support grant. Stephanie Scheemaeker was funded by the Special Research Fund of Ghent University (BOF19/DOC/015) and a travel grant from the Research Foundation - Flanders (FWO) (grant number 76 111).

### **Ethical statement**

No ethical approval was obtained because all five thyroid masses were surgically removed for treatment and diagnostic purposes. Only left-over tissue samples of the five thyroid masses were used for research purposes.

**Conflict of interest**

The authors declare no conflicts of interest.

**Data availability statement**

The data that support the findings of this study are available from the corresponding author upon reasonable request.

**Corresponding author**

Stephanie Scheemaeker

Salisburylaan 133, 9820 Merelbeke, Belgium

stephanie.scheemaeker@ugent.be

+32 9 264 77 00

**List of abbreviations**

*	frozen organoids
AddF <sup>+++</sup>	advanced DMEM/F12 containing HEPES, L-glutamine and penicillin/streptomycin
BAF	B-allele frequency
BME	basement membrane extract
c	canine
COX-2	cyclooxygenase-2
CTB	cell titer blue
DMEM	Dulbecco's Modified Eagle Medium
DMSO	dimethylsulfoxide

F	female
FN	female neutered
FTC	follicular cell thyroid carcinoma
FBS	fetal bovine serum
HE	hematoxylin and eosin
IBD	identity-by-descent
IHC	immunohistochemistry
LI	labeling index
LRR	logR ratio
MC	mitotic count
MN	male neutered
MTC	medullary thyroid carcinoma
NA	not available
P	passage
PBS	phosphate buffered saline
PFA	paraformaldehyde
R	receptor
RT	room temperature
SNP	single nucleotide polymorphism
TC	thyroid carcinoma
TKI	tyrosine kinase inhibitor
TOC	toceranib phosphate
TT4	total thyroxine
TTF-1	thyroid specific transcription factor-1

VEGF           vascular endothelial growth factor  
VEGFR         vascular endothelial growth factor receptor

Word count: 4405

Number of tables: 4

Number of figures: 8

## Abstract

Organoid cultures could constitute a valuable *in vitro* model to explore new treatments for canine (c) medullary thyroid carcinoma (MTC). The study's objectives were to establish and characterize 3D organoid cultures of cMTC using histology and immunohistochemistry (IHC) and to evaluate the effect of antitumor drugs on organoids' viability. Five cMTC tissue samples were used to develop organoid cultures of which one organoid line, named cMTC N°2, could be passaged for an extended period. This cMTC N°2 organoid line was further compared to the primary tumor regarding morphology and IHC expression of thyroid transcription factor-1 (TTF-1), thyroglobulin, calcitonin, synaptophysin, vimentin, Ki-67, cyclooxygenase-2 (COX-2), P-glycoprotein and vascular endothelial growth factor (VEGF). Quality control of the cMTC N°2 organoid line was achieved by a single nucleotide polymorphism (SNP) array of the organoids, primary tumor and healthy blood cells of the same dog. The effect of carboplatin, meloxicam and toceranib phosphate (TOC) on cMTC N°2 organoids' viability was evaluated. The cMTC N°2 organoid line was cultured for 94 days and showed similar histological features with the primary tumor. Immunolabeling for TTF-1, thyroglobulin, calcitonin and VEGF was similar between the primary tumor and cMTC N°2 organoids. Compared to the primary tumor, organoids showed higher immunolabeling for vimentin and Ki-67, and lower immunolabeling for synaptophysin, COX-2 and P-glycoprotein. The SNP genotype was similar for each chromosome between healthy blood cells, primary tumor and cMTC N°2 organoids. Carboplatin, meloxicam and TOC had no effect on cMTC N°2 organoid cell viability within achievable *in vivo* concentration range. In conclusion, the cMTC N°2 organoid line is a promising first milestone towards an established *in vitro* organoid model to explore pathophysiology and new treatment modalities in cMTC.

**Keywords:** cell culture techniques, dogs, histology, immunohistochemistry, neoplasms, thyroid carcinoma

## Introduction

In dogs, 90% of thyroid tumors detected clinically are carcinomas.<sup>1,2</sup> Of these, 30% arise from the parafollicular cells and 70% from the thyroid follicular cells, called medullary thyroid carcinoma (MTC) and follicular cell thyroid carcinoma (FTC), respectively.<sup>2</sup> Canine (c) MTC and FTC of compact type have similar histological appearance. Therefore, immunohistochemistry (IHC) for thyroglobulin, calcitonin or neuroendocrine markers (e.g., synaptophysin) helps to differentiate them reliably.<sup>3,4</sup>

To date, studies on biological behavior and treatment outcome of cMTCs are scarce. Treatment options include thyroidectomy, radiotherapy, chemotherapy and tyrosine kinase inhibitors (TKIs). One study reported that cMTCs are less invasive, seeming more amenable to surgical resection, and show fewer metastases at diagnosis compared to cFTCs.<sup>5</sup> However, following thyroidectomy, prognosis is comparable between both tumor types.<sup>6</sup> Unfortunately, thyroidectomy is precluded in up to 50-75% of canine thyroid carcinomas (TCs) due to invasive growth.<sup>1</sup> Although, radiotherapy is an excellent treatment alternative, its availability is limited. Therefore, systemic treatment options, such as chemotherapy and TKIs, remain important in the therapeutic management of cMTCs. The need for further research into systemic therapeutic modalities is further reinforced by the invasive growth and high metastatic rate of cTCs.<sup>1</sup> Although, the results of chemotherapy have been largely disappointing, recent reports indicate that TKIs (e.g., toceranib phosphate (TOC)) are associated with significant clinical benefit in dogs with TC, particularly in dogs with incompletely excised, recurrent and/or metastatic TC.<sup>1,2,7,8</sup> Unfortunately, no studies have yet been performed specifically on cMTCs. Cyclooxygenase-2 (COX-2), P-glycoprotein and vascular endothelial growth factor (VEGF)/VEGF receptor (VEGFR) have been proposed to be promising therapeutic targets in cMTCs, but to date, no studies have evaluated the therapeutic potential of COX-2 inhibitors in cTCs.<sup>9,10</sup> Both, COX-2 inhibitors and TKIs, have also been shown to inhibit the expression and function of P-glycoprotein, which is an important cause of chemoresistance.<sup>11-13</sup> The development of an

adequate *in vitro* model of cMTC could help elucidate the therapeutic value of COX-2 inhibitors and TKIs prior to clinical trials.

Organoids are 3D cell culture systems derived from stem cells capable of self-organization and self-renewal, which maintain the *in vivo* tissue architecture and function, making it possible to model clinically relevant drug responses.<sup>14</sup> Canine organoid cultures have been established from normal and/or neoplastic bladder, epidermis, intestines, kidney, liver, mammary glands and prostate.<sup>15-23</sup> Recently, our group established organoids from naturally occurring FTC in dogs.<sup>24</sup> Organoids of cMTC could be beneficial to explore new treatment strategies before investing in clinical trials. To date, organoids of naturally occurring MTC have not been established in any species.

The objectives of this study were to establish organoid cultures of cMTC, to characterize them using histology and IHC, and to perform single nucleotide polymorphism (SNP) genotyping as a quality control. Furthermore, proliferation assays were performed to evaluate the effect of several antitumor drugs on cMTC organoid viability. The chemotherapeutic carboplatin, the COX-2 inhibitor meloxicam and the TKI TOC were selected based on their clinical use in cTCs.

## Methods

### Tissue samples

Samples from five cMTCs were obtained from the biobank of canine thyroid tumor tissue of the Vetsuisse Faculty (University of Bern).<sup>24</sup> The tissue samples originated from client-owned dogs with naturally occurring MTC, collected after thyroidectomy for diagnostic and curative purposes. Therefore, no approval of the Ethical Committee was obtained.

Half of the surgically removed thyroid mass was fixed in 10% buffered formalin followed by paraffin-embedding and subsequently histopathology. The remaining half, stored at 4°C in Dulbecco's Modified Eagle Medium (DMEM; Thermo Fisher Scientific, Waltham, MA, USA) with 1% penicillin/streptomycin (Thermo Fisher Scientific), was processed within 12 h and reserved for research purposes. Therefore, tissue



was washed in phosphate buffered saline (PBS), cut in 5 mm pieces and largely stored in freezing medium containing 45% DMEM (Thermo Fisher Scientific), 45% fetal bovine serum (FBS; Thermo Fisher Scientific) and 10% dimethylsulfoxide (DMSO; Merck Millipore, Darmstadt, Germany) at -150°C. Corresponding EDTA-anticoagulated whole blood and remaining tumor tissue pieces were also frozen at -80°C and snap frozen in liquid nitrogen, respectively.

Dogs were staged using the WHO TNM staging system for canine thyroid tumors (Table 1).<sup>25</sup>

### Organoid culture

Frozen tissue pieces of the five cMTCs were washed and centrifuged (5 min, 300 g) twice separately with advanced DMEM/F12 (Thermo Fisher Scientific) containing HEPES (10 mM; Sigma Aldrich, Saint Louis, MO, USA), L-glutamine (2 mM; Thermo Fisher Scientific) and penicillin/streptomycin (50 U/mL; Thermo Fisher Scientific) (AdDF<sup>+++</sup>). Tissue pieces were enzymatically dissolved in collagenase type IV (2 mg/mL; Sigma Aldrich) and Y-27632 dihydrochloride (1.65 μM; Abmole Bioscience, Houston, TX, USA) (30 min, 37°C). Tissue suspensions were filtered using a 100-μm nylon mesh (Thermo Fisher Scientific) to retain single cells and small cell clusters. The filtered cell suspensions were centrifuged (5 min, 460 g) twice and the cell pellets were resuspended in basic growth medium containing 75% AdDF<sup>+++</sup>, 10% conditioned R-Spondin medium (in-house), 10% conditioned Noggin medium (in-house), 2% serum-free B-27 supplement (Thermo Fisher Scientific) and bovine TSH (8 mIU/mL; Sigma Aldrich) as main components (Supplementary material 1). The cell suspension with basic growth medium was mixed with Cultrex<sup>®</sup> basement membrane extract (BME; R&D Systems, Minneapolis, MN, USA) on ice in a 1:1 ratio to create 30 μL droplets on pre-warmed 24-well plates. After 30 min incubation (5% CO<sub>2</sub>, 37°C), pre-warmed basic growth medium per well was added to the solidified droplets. Culture conditions were 5% CO<sub>2</sub> and 37°C. Basic growth medium was refreshed twice weekly. Organoids were reseeded or passaged every 3-6 and 7-14 days, respectively.

Organoids were passaged by enzymatic dissociation with TrypLE Express (1X, Thermo Fisher Scientific) (10 min, 37°C) followed by mechanical disruption.

Organoids' growth and appearance were microscopically evaluated every 2-3 days.

One of the five cMTC cultures, named cMTC N°2, could be passaged for a longer time in culture. Henceforth, only this organoid line will be referred to in this study.

#### Freezing and storage

Five days after passaging, small to medium sized organoids (20-125 µm) were frozen. Therefore, organoids were resuspended in basic growth medium and Recovery™ cell culture freezing medium (Thermo Fisher Scientific) in a 1:1 ratio. The whole was stored in cryogenic tubes (Thermo Fisher Scientific) and slowly frozen at -80°C in a freezing container (Nalgene® Mr. Frosty; Sigma Aldrich). After 24 h, organoids were transferred to -150°C.

#### Embedding

Organoids were incubated for 2 h in 4% paraformaldehyde (PFA) at room temperature (RT). The PFA-fixed organoid pellets were then resuspended in pre-warmed 2.5% agarose solution and placed in pre-warmed histology molds. After cooling the agarose-organoid pellets (10 min, 4°C), the pellets were placed in histology cassettes. The latter were incubated consecutively in 50% ethanol (1 h, RT), 80% ethanol (2 h, 4°C) and 4% PFA (12 h, RT). The formalin-fixed organoid pellets were then paraffin-embedded and cut. Subsequently, slides were prepared for hematoxylin and eosin (HE) staining and IHC.

#### Histology

Histological analysis of all five primary tumors and the cMTC N°2 organoid line was performed by a board-certified pathologist (MD). The evaluated histological criteria were cell morphology, cell organization (i.e.,

follicular, compact, follicular-compact), mitotic count (MC) (evaluated in 10 high-power fields, 400x magnification), and presence of anisocytosis and anisokaryosis. Histologic type of primary tumors was determined according to the WHO's histological classification system for canine thyroid tumors.<sup>26</sup> Classification of cMTCs was also based on positive immunolabeling for calcitonin.

### Immunohistochemistry

Three µm sections of the formalin-fixed paraffin-embedded blocks of the primary tumors and cMTC N°2 organoid line were prepared on positively charged glass slides (Color Frosted Plus; Biosystems, Muttenz, Switzerland). Immunohistochemistry for thyroid transcription factor-1 (TTF-1), thyroglobulin, calcitonin, synaptophysin, vimentin and Ki-67 was performed using a Bond-III automated immunostainer (Leica Biosystems, Wetzlar, Germany) at Pathologie Länggasse (Ittigen, Switzerland) according to manufacturer's instructions (Table 2).<sup>4</sup> Immunohistochemistry for COX-2, P-glycoprotein and VEGF was performed as previously described by our group at the Department of Pathobiology, Pharmacology and Zoological Medicine (Ghent University) (Table 2).<sup>9</sup> Minor modifications to the protocol were reduction of microwave time to 3.5 min (850 W) and 10 min (300 W) in the antigen retrieval step and incubation step with the primary antibodies at RT, respectively.

Positive controls were stained in parallel with the respective antibody (Table 2). Negative controls were obtained by replacing each primary antibody by 2% dog serum (LabForce, Muttenz, Switzerland).

All sections were evaluated by a board-certified pathologist (MD). The percentage of positive immunolabeled cells was subjectively estimated, except for Ki-67. Ki-67 positive cells were quantified by calculation of the Ki-67 labeling index (LI). Therefore, a photomicrograph at 400x magnification was taken of the two regions with seemingly the highest number of Ki-67-positive cells, in both the primary tumor and organoids. In the primary tumor, the total number of tumor cells was counted using the image

processing program Fiji (Image J).<sup>27</sup> Ki-67-positive tumor cells of the primary tumor, and the total number of organoid cells and Ki-67-positive organoid cells were counted manually. Ki-67 LI was calculated as the number of Ki-67-positive cells divided by the total number of cells. The highest Ki-67 LI from the two regions was selected for both the primary tumor and the organoids.

#### Cell viability and proliferation assays

Organoids were incubated in growth medium containing different concentrations of carboplatin (0, 5, 10, 25, 35, 60 and 120  $\mu$ M) (Carboplatin-Teva<sup>®</sup> liquid 50 mg/5mL; Teva Pharma AG, Basel, Switzerland), meloxicam sodium salt hydrate (0, 20, 40, 80, 120 and 160  $\mu$ M) (M3935; Sigma Aldrich) and TOC (0, 150, 300, 600, 900 and 1200 nM) (PZ0338; Sigma Aldrich). The evaluated *in vitro* drug concentrations were derived from canine and human 2D cell culture studies.<sup>28-30</sup> Prior to preparation of the drug-containing growth media, carboplatin was dissolved in basic growth medium (2.70 mM solution), whereas meloxicam and TOC were dissolved separately in DMSO (26.78 mM and 5.05 mM solutions, respectively) according to manufacturer's instructions. Additionally, DMSO was added to the growth medium of each condition (control group and treatment groups) in the proliferation assays of meloxicam and TOC to obtain a final .6% and .02% solution, respectively. Two replicates of each proliferation assay (i.e., carboplatin, meloxicam and TOC) were conducted in which each condition (control group and treatment groups) was represented by three wells.

Organoids were enzymatically dissociated with TrypLE Express (1X, Thermo Fisher Scientific) (20 min, 37°C) and filtered using a 40- $\mu$ m cell strainer (Corning, New York, NY, USA) to obtain single organoid cells. Cells were washed and centrifuged (5 min, 470 g) to collect the cell pellet. Thirty- $\mu$ L droplets of basic growth medium and BME (R&D Systems) in a 1:1 ratio, containing 150 000 single cells, were created on pre-warmed 24-well plates and incubated (30 min, 37°C). Pre-warmed growth media with the different concentrations of each drug were added separately to each well. Three wells per condition (control and

treatment groups) were incubated (5% CO<sub>2</sub>, 37°C). Growth medium of control and treatment groups was replaced with basic growth medium after 24 h (carboplatin) or 48 h (meloxicam, TOC). Basic growth medium was refreshed every 2 days until the end of the proliferation assays (day 10).

Organoid cells' viability was monitored using CellTiter-Blue® (CTB) cell viability assays (Promega; Madison, WI, USA) at days 7 (meloxicam, TOC) and 8 (carboplatin), and day 10 of the proliferation assays. Therefore, basic growth medium was removed and replaced by CTB reagent in pre-warmed AdDF<sup>+++</sup> in a 1:20 ratio. After 4 h of incubation (5% CO<sub>2</sub>, 37°C), 200 µL of each well was pipetted in a 96-well plate and fluorescence signal, emitted by the fluorophore produced by viable organoid cells, was read by a multimode plate reader with a 560 nm excitation/590 nm emission filter set (EnSpire™ 2300; PerkinElmer, Waltham, MA, USA).<sup>31</sup> After the first CTB assay (days 7 or 8), medium was replaced by basic growth medium. After the second CTB assay (day 10), organoids of the zero and two highest concentrations of each drug were embedded separately for histology and IHC.

Data were plotted in three separate dose response curves where the x-axis indicates the drug concentration (i.e., carboplatin, meloxicam and TOC) and the y-axis indicates the % cell viability of the organoid cells, measured at day 7 (meloxicam, TOC) or day 8 (carboplatin), and day 10 (Fig. 1). The % cell viability was calculated by normalizing the fluorescence signal emitted by the fluorophore produced by the viable organoid cells to the fluorescence signal emitted by the fluorophore produced by the untreated viable organoid cells (control group).

#### DNA extraction

DNA was extracted from EDTA-anticoagulated whole blood (healthy cells), snap frozen primary tumor and organoids of the same dog. Prior to DNA extraction, tumor tissue was washed with PBS, a stainless-steel

bead was added and the whole was placed in the TissueLyser (QIAGEN, Hilden, Germany) for 2 min. Thereafter, DNA from the tissue lysate and whole blood was extracted using the QIAamp® DNA mini kit (QIAGEN) and the QIAamp® DNA blood mini kit (QIAGEN), respectively, according to the manufacturer's instructions. A chloroform-based DNA extraction method was used to extract DNA from the organoids. DNA quality and concentration were measured using NanoDrop® ND-1000 spectrophotometer (Thermo Fisher Scientific). DNA quality was quantified using the 260/280 absorbance ratio.

#### Single nucleotide polymorphism genotyping array

Extracted DNA from healthy cells, primary tumor and organoids of the same dog was genotyped using the Illumina CanineHD BeadChip array (Illumina, San Diego, CA, USA) (Neogen, Lincoln, NE, USA). Data were quality-filtered and analyzed with PLINK v1.9 software.<sup>32</sup> Confirmation of sample identity and sex based on heterozygosity rates, and detection of possible sample contamination, swaps or duplications based on pairwise identity-by-descent (IBD) estimation were performed. Subsequently, a combination of two SNP genotyping array measures, B-allele frequency (BAF) and logR ratio (LRR), was plotted per chromosome in the healthy cells, primary tumor and organoids of the same dog using RStudio v3.6.0.<sup>33</sup> Plots from the same chromosome were compared visually between healthy cells, primary tumor, and organoids to detect potential differences.

#### Cell line validation statement

The cMTC N°2 organoid line was validated by histology and IHC as described in this manuscript. A SNP genotyping array of both organoids, respective primary tumor and healthy cells was performed as a quality control of the derived organoid line.

#### Statistical analysis

The difference in cell viability between organoids incubated with different concentrations of the same drug (i.e., carboplatin, meloxicam and TOC) was compared using a repeated measures ANOVA. Significance level was defined at .05.

## Results

### cMTC cultures

Five cMTCs were used to develop organoid cultures (Table 1). Thyroid function status, TNM classification and tumor stage of each dog are detailed in Table 1.

One organoid line (cMTC N°2) could be reseeded and passaged for 94 days (passage (P) 9) until the end of the study (Table 1, Fig. 2). The cMTC N°2 organoids grew slowly though continuously. The remaining four cMTC cultures were discontinued due to absent growth (n=3) or bacterial contamination (n=1) (Table 1).

Two times six and 24 wells of cMTC N°2 organoids were frozen and stored at P5 (43 days), P7 (69 days) and P9 (94 days), respectively. To evaluate organoids' viability after freezing, organoids frozen at P5 were brought to culture after 25 days and were cultured for another 28 days (P7\*), until the end of the study.

Only the results of the cMTC N°2 organoids are further described and discussed.

Microscopically, organoids were roundish to ovoid in shape with a cystic to solid appearance and a thickened wall (Fig. 2). Organoids' size was independent of age (Fig. 2).

### Histology and IHC

Primary thyroid tumor and organoids (P4, 37 days; P8, 84 days) were characterized by histology and/or IHC for TTF-1, thyroglobulin, calcitonin, synaptophysin, vimentin, Ki-67, COX-2, P-glycoprotein and/or VEGF (Tables 3-4, Figs. 3-6). The positive control tissue and negative control, which were stained in parallel with the tissue of interest (i.e., primary tumor and organoids), labeled positive and negative, respectively, for each evaluated antibody.

The primary tumor showed a compact organization of polygonal cells with a moderate grade of anisocytosis and anisokaryosis (Fig. 3A). Follicular structures were absent. The MC of the primary tumor was 5. Organoids (P4) also had a compact organization of polygonal cells without follicular organization (Fig. 3B). A moderate to high grade of anisocytosis and anisokaryosis was observed (Fig. 3B). The MC of the organoids (P4) was 0. The organoids (P8) of the different treatment groups showed a similar morphology with each other and with the untreated organoids (P4). In the control group of TOC (P8 0nM TOC) some organoid cells showed a follicular organization next to compactly organized cells, and MC was 3 (Fig. 3C). At the highest concentrations of carboplatin, meloxicam and TOC, vacuolization of some organoid cells was observed.

Both primary tumor and organoids (P4, P8 0 nM TOC) showed positive immunolabeling for TTF-1 and negative immunolabeling for thyroglobulin (Table 3, Figs. 4-6). Primary tumor and organoids (P8 0 nM TOC) showed positive immunolabeling for calcitonin and synaptophysin, which was negative in the organoids at P4 (Table 3) (Figs. 4-6). Compared to the primary tumor, synaptophysin, COX-2 and P-glycoprotein immunolabeling were lower, while vimentin immunolabeling and Ki-67 LI were higher in the organoids (P4, P8) (Table 3, Figs. 4-6). Both, primary tumor and organoids (P4, P8 0 nM TOC), showed a similar high percentage of VEGF-positive cells (Table 3). Drug type and concentration seemed not to influence immunolabeling for COX-2, P-glycoprotein and VEGF in organoid cells (P8) (Table 4).

#### SNP genotyping array

Extracted DNA from healthy cells, primary tumor and organoids (P7) was genotyped.

PLINK data showed that the proportion of IBD between the different samples was  $> .99$ , confirming their same origin. Also, analysis of the X-chromosome SNPs of the samples were in agreement with male origin ( $F > .84$ ). Additionally, both BAF and LRR plots showed no obvious differences in SNPs per chromosome between the healthy cells, primary tumor and organoids (Figs. 7-8).



### Anti-cancer drug response

Proliferation assays were performed on organoids at P8 and P9 to obtain two replicates for each drug. No significant differences were observed in % cell viability of the cMTC N°2 organoid cells incubated with different concentrations of each drug ( $P > .32$ ) (Fig. 1). From day 8-10 and day 7-10, % cell viability changed (i.e., increase or decrease) regardless of drug type and concentration (Fig. 1).

### **Discussion**

We described the first organoid line of naturally occurring MTC from any species. The cMTC organoid line was characterized by an adequate and stable proliferative capacity considering the long-term viable culture, the moderate to high Ki-67 LI and continued growth after freezing.

Histology of cMTC organoid cells showed a similar morphology and organization as the primary tumor cells, with the exception of the follicle-like structures in the organoids at P8, which somewhat contrast with the compact architecture of MTC.<sup>34</sup> The positive immunolabeling of the cMTC organoids for TTF-1, calcitonin and synaptophysin confirmed their thyroid, C-cell and neuroendocrine origin, respectively.<sup>3,4</sup> This was further supported by the negative immunolabeling for thyroglobulin.

Although the cMTC N°2 organoid line had an adequate proliferative activity, the MC was rather low in the evaluated passages (i.e., P4 and P8) in comparison to the primary tumor. However, the Ki-67 LI, which was higher in the organoids compared to the primary tumor, is preferred over the MC as proliferative marker as the Ki-67 LI is a graded marker for all the active phases of the cell cycle (i.e., G1, S, G2 and mitosis) while the MC is rather a binary marker for only the mitosis phase of the cell cycle.<sup>35,36</sup> Also, in sparsely cellular sections, such as our cMTC N°2 organoids, the MC gives a less adequate representation of the number of mitotic figures in comparison to sections with dense cellularity such as our primary tumor.<sup>37</sup> Hence, the Ki-

67 LI better represents the proliferative activity of our cMTC N°2 organoid line than the MC. The reason for the lower Ki-67 LI in the organoids at P8 compared to P4 is unclear.

The SNP genotyping of healthy cells, primary tumor, and organoids confirmed samples' identity and absence of sample contamination, swaps or duplications by observing the high proportion of IBD between samples, the male origin of samples, and the similar BAF and LRR per SNP on each chromosome. Furthermore, no promising therapeutic molecular targets were identified with this simplified genetic comparison between the healthy cells and primary tumor based on the close similarity of the BAF and LRR plots.

Differences in immunolabeling for calcitonin, synaptophysin, vimentin, COX-2 and P-glycoprotein were observed between the primary tumor, organoids at P4 and organoids at P8. A possible insufficient differentiation of the organoid cells could explain these differences. It is well known that calcitonin and synaptophysin are important differentiation markers for thyroid C-cells and neuroendocrine cells (i.e., thyroid C-cells), respectively, while vimentin, a marker of mesenchymal cells, is more expressed in immature cells or with an increased cellular activity.<sup>3,4,38</sup> This is supported on the one hand by the high percentage of vimentin-positive organoid cells (P4, P8) compared to 10% of primary tumor cells, and on the other hand by the increased immunolabeling for calcitonin, synaptophysin, COX-2 and P-glycoprotein, and the decreased immunolabeling for vimentin of organoid cells from P4 (37 days) to P8 (83 days). Optimization of our organoids' protocol, and to a lesser extent longer time in culture, might allow better preservation of primary tumor characteristics and further differentiation of cMTC organoid cells during culture.

To date, traditional treatment modalities are inadequate (i.e., thyroidectomy and radiotherapy) or unsuccessful (i.e., chemotherapy) to treat metastatic cMTC.<sup>1,2</sup> Previous studies have shown that COX-2, P-glycoprotein and VEGF/VEGFR could constitute promising therapeutic targets in cMTCs, but to date, no *in vitro* models were available to investigate this further.<sup>9,10</sup> Two clinical studies evaluated the response of cTC to TOC and up to 88% of dogs experience clinical benefit.<sup>7,8</sup> It is not clear so far if clinical benefit is associated with tumor type (i.e., cFTC and cMTC) and/or presence of molecular targets for TOC. In our study, the effects of COX-2 inhibitor meloxicam and TKI TOC on cMTC organoid cells' viability were evaluated separately. The lack of effect of meloxicam on cMTC organoid cells' viability could be explained by their low expression of COX-2. Furthermore, TOC also had no inhibitory effect on cMTC organoids cells' viability, which showed positive VEGF immunolabeling. The anti-angiogenic effect of TOC is exerted by inhibiting the VEGFR and platelet-derived growth factor receptor, while its direct antitumor effect likely originates from inhibiting other tyrosine kinases.<sup>13,39,40</sup> Since blood vessels and angiogenesis are lacking in organoid culture models, the anti-angiogenic effect of TOC in our cMTC organoid line could not be assessed.<sup>14</sup> A possible explanation for the lack of effect of TOC on our cMTC organoid cells' viability could be an insufficient incubation time of the organoids with TOC. To date, no proliferation assays with TOC have been published in organoid cultures. The technical data (i.e., TOC concentration and incubation time) in our proliferation assay was derived from a proliferation study with 2D neoplastic mammary cell lines.<sup>28</sup> Due to the 3D organization of organoids, it could be that organoids require longer incubation times compared to 2D cultures.

The effect of chemotherapy to treat cTCs has been disappointing, both as mono- and adjuvant therapy.<sup>1,2</sup> Expression of P-glycoprotein, a multidrug efflux pump that increases efflux of chemotherapeutics, thereby lowering their intracellular concentration and toxicity, could be one of the possible mechanisms for this chemoresistance.<sup>41</sup> P-glycoprotein is expressed in cTCs, especially in cMTCs.<sup>9</sup> In our study however, no

decrease of cMTC organoids' viability was observed with carboplatin, despite the low P-glycoprotein immunolabeling. This could suggest that chemoresistance of cMTCs may be associated with other mechanisms. Studies on chemoresistance in cMTCs, and in cTCs in general, are lacking and cTC organoids could constitute an ideal research model to further explore these mechanisms and develop therapeutic strategies to circumvent them.

The main limitation of our study is the low number of cultured cMTCs. Long-term organoid culture was established in only one cMTC. Modification of the culture protocol in future studies may improve the success rate of cMTC organoid cultures. Concretely, changing the concentrations of the used growth media components and/or adding extra growth factors, such as Wnt-3a and fibroblast growth factor, to our basic growth medium, could potentially enhance cMTC organoids' growth and differentiation.<sup>42-44</sup>

Another limitation is the fact that histology and IHC of cMTC organoids at P8 were obtained from the control groups of the proliferation assays with meloxicam and/or TOC. The P8 organoid cells of these control groups were temporarily incubated in a .6 and .02% solution of basic growth medium with DMSO. However, we do not expect the low concentrations of DMSO in the culture media of P8 organoids to have a major effect on our results.

In conclusion, we developed the first organoid line of primary MTC in any species. Further optimization of organoid culture conditions is warranted in future studies. Canine MTC organoids could constitute a promising *in vitro* model to gain insight into new treatment modalities for cMTC in advance of clinical studies.

## References

1. Scott-Moncrieff JC. Canine thyroid tumors and hyperthyroidism. In: Feldman EC, Nelson RW, Reusch CE, Scott-Moncrieff JCR, eds. *Canine and Feline Endocrinology*. 4th ed. St. Louis, MO: W.B. Saunders; 2015:196-212.
2. Ward CR. Canine hyperthyroidism. In: Ettinger SJ, Feldman EC, Côté E, eds. *Textbook of Veterinary Internal Medicine Expert Consult*. 8th ed. St. Louis, MO: Elsevier; 2017:1757-1761.
3. Erickson LA, Lloyd RV. Practical markers used in the diagnosis of endocrine tumors. *Adv Anat Pathol*. 2004;11(4):175-189.
4. Ramos-Vara JA, Miller MA, Johnson GC, Pace LW. Immunohistochemical detection of thyroid transcription factor-1, thyroglobulin, and calcitonin in canine normal, hyperplastic, and neoplastic thyroid gland. *Vet Pathol*. 2002;39(4):480-487.
5. Carver JR, Kapatkin A, Patnaik AK. A comparison of medullary-thyroid carcinoma and thyroid adenocarcinoma in dogs - a retrospective study of 38 cases. *Vet Surg*. 1995;24(4):315-319.
6. Campos M, Ducatelle R, Rutteman G, et al. Clinical, pathologic, and immunohistochemical prognostic factors in dogs with thyroid carcinoma. *J Vet Intern Med*. 2014;28(6):1805-1813.
7. Sheppard-Olivares S, Bello NM, Wood E, et al. Toceranib phosphate in the treatment of canine thyroid carcinoma: 42 cases (2009-2018). *Vet Comp Oncol*. 2020;18(4):519-527.
8. London C, Mathie T, Stingle N, et al. Preliminary evidence for biologic activity of toceranib phosphate (Palladia (R)) in solid tumours. *Vet Comp Oncol*. 2012;10(3):194-205.
9. Campos M, Ducatelle R, Kooistra HS, et al. Immunohistochemical expression of potential therapeutic targets in canine thyroid carcinoma. *J Vet Intern Med*. 2014;28(2):564-570.
10. Urie BK, Russell DS, Kisseberth WC, London CA. Evaluation of expression and function of vascular endothelial growth factor receptor 2, platelet derived growth factor receptors-alpha and -beta, KIT, and RET in canine apocrine gland anal sac adenocarcinoma and thyroid carcinoma. *BMC Vet Res*. 2012;8.
11. Zatelli MC, Luchin A, Piccin D, et al. Cyclooxygenase-2 inhibitors reverse chemoresistance phenotype in medullary thyroid carcinoma by a permeability glycoprotein-mediated mechanism. *J Clin Endocrinol Metab*. 2005;90(10):5754-5760.
12. Zandvliet M, Teske E, Chapuis T, Fink-Gremmels J, Schrickx JA. Masitinib reverses doxorubicin resistance in canine lymphoid cells by inhibiting the function of P-glycoprotein. *J Vet Pharmacol Ther*. 2013;36(6):583-587.
13. Elfadadny A, El-Husseiny HM, Abugomaa A, et al. Role of multidrug resistance-associated proteins in cancer therapeutics: past, present, and future perspectives. *Environmental Science and Pollution Research*. 2021;28(36):49447-49466.
14. Iakobachvili N, Peters PJ. Humans in a dish: the potential of organoids in modeling immunity and infectious diseases. *Frontiers in Microbiology*. 2017;8.
15. Chandra L, Borcharding DC, Kingsbury D, et al. Adult canine intestinal derived organoids: a novel in vitro system for translational research in comparative gastroenterology. *bioRxiv*. 2018:466409.
16. Elbadawy M, Usui T, Mori T, et al. Establishment of a novel experimental model for muscle-invasive bladder cancer using a dog bladder cancer organoid culture. *Cancer Sci*. 2019;110(9):2806-2821.
17. Schotanus BA, Spee B, Nantasanti S, et al. Establishment of Genetically Stable Canine Liver Organoids for Translational Studies. *Tissue Engineering Part A*. 2015;21:S8-S8.
18. Chen TC, Neupane M, Chien SJ, et al. Characterization of adult canine kidney epithelial stem cells that give rise to dome-forming tubular cells. *Stem Cells Dev*. 2019;28(21):1424-1433.
19. Cocola C, Molgora S, Piscitelli E, et al. FGF2 and EGF are required for self-renewal and organoid formation of canine normal and tumor breast stem cells. *J Cell Biochem*. 2017;118(3):570-584.

20. Usui T, Sakurai M, Nishikawa S, et al. Establishment of a dog primary prostate cancer organoid using the urine cancer stem cells. *Cancer Sci.* 2017;108(12):2383-2392.
21. Wiener DJ, Basak O, Asra P, et al. Establishment and characterization of a canine keratinocyte organoid culture system. *Vet Dermatol.* 2018;29(5):375-+.
22. Elbadawy M, Fujisaka K, Yamamoto H, et al. Establishment of an experimental model of normal dog bladder organoid using a three-dimensional culture method. *Biomedicine & Pharmacotherapy.* 2022;151:113105.
23. Inglebert M, Dettwiler M, Hahn K, et al. A living biobank of canine mammary tumor organoids as a comparative model for human breast cancer. *Scientific Reports.* 2022;12(1):18051.
24. Jankovic J, Dettwiler M, Fernandez MG, et al. Validation of immunohistochemistry for canine proteins involved in thyroid iodine uptake and their expression in canine follicular cell thyroid carcinomas (FTCs) and FTC-derived organoids. *Vet Pathol.* 2021;58(6):1172-1180.
25. Owen LN, Organization. WH. TNM classification of tumours in domestic animals/ edited by L.N. Owen. In. Geneva: World Health Organization; 1980.
26. Kiupel M. *Histological classification of tumors of the endocrine system of domestic animals.* Washington, DC: Armed Forces Institute of Pathology in cooperation with the CL Davis DVM Foundation and the World Health Organization Collaborating Center for Worldwide Reference on Comparative Oncology; 2008.
27. Schindelin J, Arganda-Carreras I, Frise E, et al. Fiji: an open-source platform for biological-image analysis. *Nat Methods.* 2012;9(7):676-682.
28. Gattino F, Maniscalco L, Iussich S, et al. PDGFR- $\alpha$ , PDGFR- $\beta$ , VEGFR-2 and CD117 expression in canine mammary tumours and evaluation of the in vitro effects of toceranib phosphate in neoplastic mammary cell lines. *Vet Rec.* 2018;183(7):221.
29. Ayakawa S, Shibamoto Y, Sugie C, et al. Antitumor effects of a cyclooxygenase-2 inhibitor, meloxicam, alone and in combination with radiation and/or 5-fluorouracil in cultured tumor cells. *Mol Med Rep.* 2009;2(4):621-625.
30. Chen J-H, Chu X-P, Zhang J-T, et al. Genomic characteristics and drug screening among organoids derived from non-small cell lung cancer patients. *Thoracic Cancer.* 2020;11(8):2279-2290.
31. Riss TL, Moravec RA, Niles AL, et al. Cell viability assays. *Assay Guidance Manual [Internet].* 2016.
32. Chang CC, Chow CC, Tellier C, Vattikuti S, Purcell SM, Lee JJ. Second-generation PLINK: rising to the challenge of larger and richer datasets. *Gigascience.* 2015;4.
33. *R: A language and environment for statistical computing* [computer program]. Vienna, Austria 2019.
34. Pineyro P, Vieson MD, Ramos-Vara JA, Moon-Larson M, Saunders G. Histopathological and immunohistochemical findings of primary and metastatic medullary thyroid carcinoma in a young dog. *J Vet Sci.* 2014;15(3):449-453.
35. Miller I, Min MW, Yang C, et al. Ki67 is a graded rather than a binary marker of proliferation versus quiescence. *Cell Reports.* 2018;24(5):1105-+.
36. Scholzen T, Gerdes J. The Ki-67 protein: from the known and the unknown. *J Cell Physiol.* 2000;182(3):311-322.
37. Thunnissen FBJM, Ambergen AW, Koss M, Travis WD, O'Leary TJ, Ellis IO. Mitotic counting in surgical pathology: sampling bias, heterogeneity and statistical uncertainty. *Histopathology.* 2001;39(1):1-8.
38. Kameda Y. Co-expression of vimentin and 19S-thyroglobulin in follicular cells located in the C-cell complex of dog thyroid gland. *J Histochem Cytochem.* 1995;43(11):1097-1106.
39. Mendel DB, Laird AD, Xin XH, et al. In vivo antitumor activity of SU11248, a novel tyrosine kinase inhibitor targeting vascular endothelial growth factor and platelet-derived growth factor

- receptors: Determination of a pharmacokinetic/pharmacodynamic relationship. *Clin Cancer Res.* 2003;9(1):327-337.
40. Bavcar S, Argyle DJ. Receptor tyrosine kinase inhibitors: molecularly targeted drugs for veterinary cancer therapy. *Veterinary and Comparative Oncology.* 2012;10(3):163-173.
  41. Gottesman MM, Fojo T, Bates SE. Multidrug resistance in cancer: Role of ATP-dependent transporters. *Nat Rev Cancer.* 2002;2(1):48-58.
  42. Lv J, Feng ZP, Chen FK, et al. M2-like tumor-associated macrophages-secreted Wnt1 and Wnt3a promotes dedifferentiation and metastasis via activating beta-catenin pathway in thyroid cancer. *Molecular Carcinogenesis.* 2021;60(1):25-37.
  43. Saito Y, Onishi N, Takami H, et al. Development of a functional thyroid model based on an organoid culture system. *Biochemical and Biophysical Research Communications.* 2018;497(2):783-789.
  44. de Lau WBM, Snel B, Clevers HC. The R-spondin protein family. *Genome Biology.* 2012;13(3):242.

Table 1: Signalment, thyroid function status, TNM classification and tumor stage of the primary cMTC patients. Time in culture, highest passage number and reason to end culture of the cMTC organoid lines are also included.

Table 2: Primary antibodies used for IHC.

Table 3: Percentage of positive cells in primary cMTC N°2 tumor and derived organoids (P4, P8) for each primary antibody used for IHC.

Table 4: Percentage of positive cells in cMTC N°2 organoids (P8) incubated with different concentrations of meloxicam (0, 120 and 160  $\mu$ M) and TOC (0, 900 and 1200 nM) for COX-2, P-glycoprotein and VEGF.



Figure 1: Dose response curves for cMTC N°2 organoids (P8) incubated for 24 h in growth medium containing different concentrations of carboplatin (0, 5, 10, 25, 35, 60 and 120  $\mu\text{M}$ ) (Fig. 1A), and 48 h in growth medium containing different concentrations of meloxicam (0, 20, 40, 80, 120 and 160  $\mu\text{M}$ ) (Fig. 1B) and TOC (0, 150, 300, 600, 900 and 1200 nM) (Fig. 1C). The x-axis indicates the drug concentration and the y-axis indicates the % cell viability of the cMTC N°2 organoid cells. Results were normalized to the control group. The % cell viability of the control groups are represented in the dose response curves by a dash dotted line at the level of a cell viability of 100% (---). The symbols represent the mean of the % cell viability of three wells per replicate of each drug concentration on day 7 (meloxicam, TOC) or 8 (carboplatin) ( $\Delta$ ), and day 10 (o). The dashed (---) and solid (—) lines connect the means of the % cell viability of both replicates per drug concentration on day 7 (meloxicam, TOC) or 8 (carboplatin), and day 10, respectively.

Figure 2: Photomicrographs of organoid line cMTC N°2, derived from a naturally occurring cMTC, at P5 (x200): A. Day 0, B. Day 3, C. Day 7, D. Day 14.

Figure 3: Photomicrographs of HE staining of cMTC N°2 (x400): A. Primary tumor, B. Organoids at P4, C. Organoids at P8 incubated with 0 nM TOC.

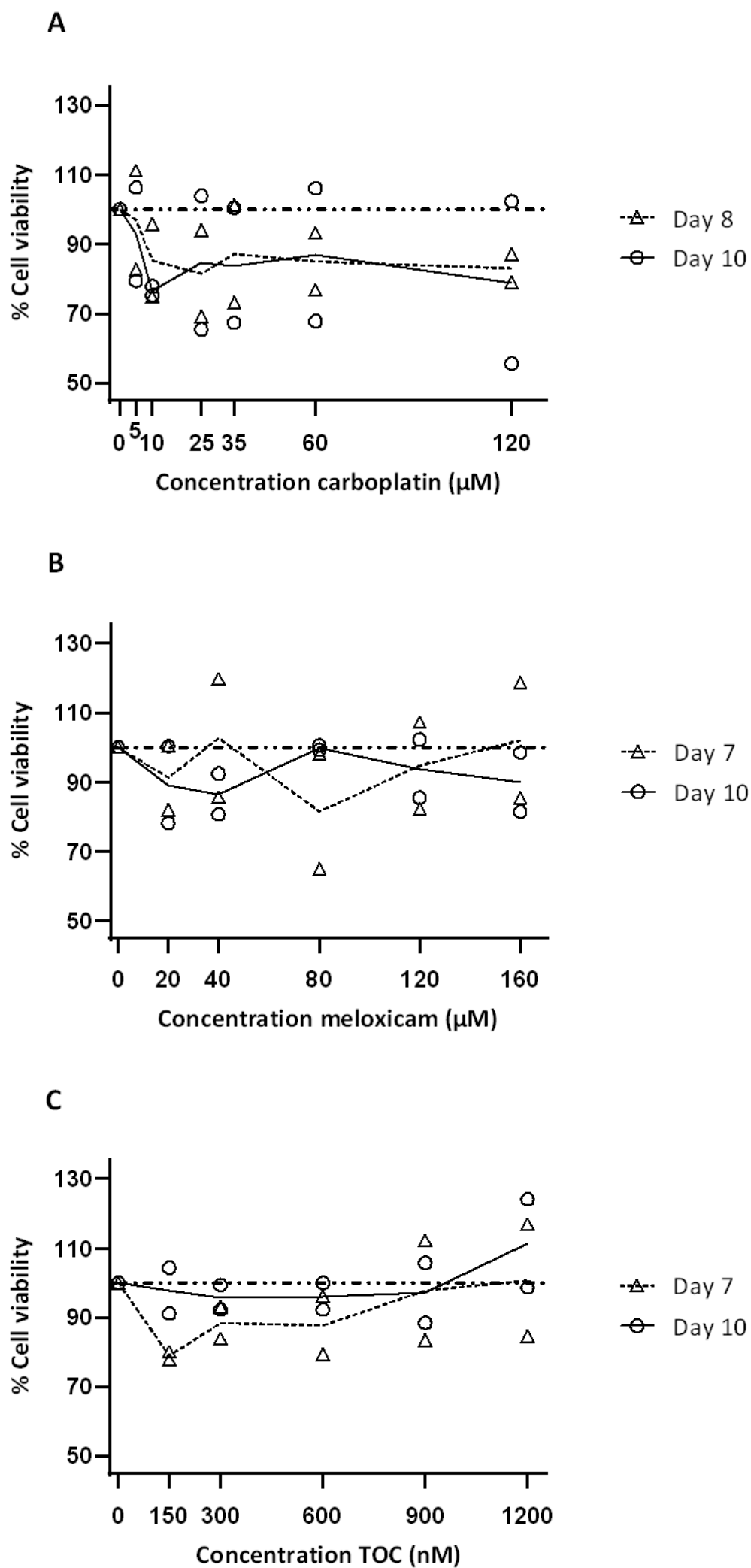
Figure 4: Photomicrographs of the cMTC N°2 primary tumor (x400): A. TTF-1 IHC staining, B. Calcitonin IHC staining, C. Synaptophysin IHC staining, D. Vimentin IHC staining.

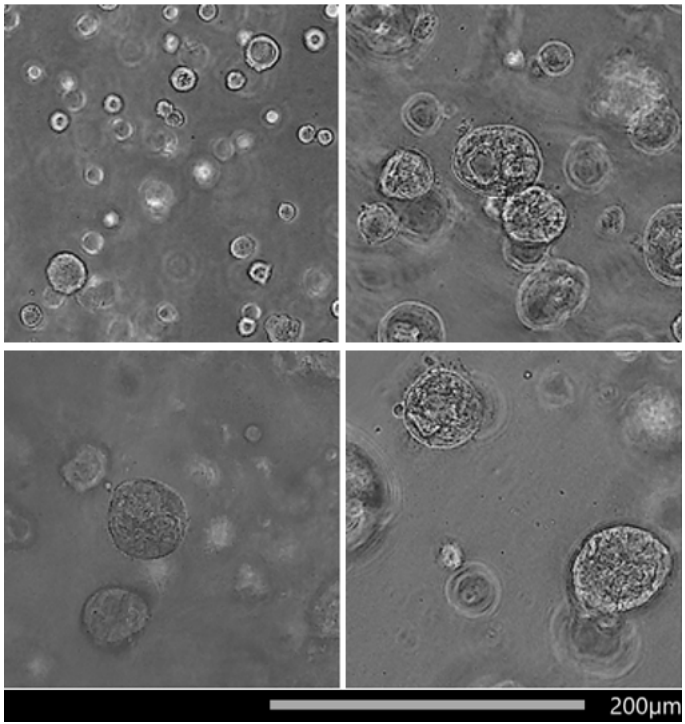
Figure 5: Photomicrographs of the cMTC N°2 organoid line, at P4 (x400): A. TTF-1 IHC staining, B. Calcitonin IHC staining, C. Synaptophysin IHC staining, D. Vimentin IHC staining.

Figure 6: Photomicrographs of the cMTC N°2 organoid line, at P8 incubated with 0 nM TOC (x400): A. TTF-1 IHC staining, B. Calcitonin IHC staining, C. Synaptophysin IHC staining, D. Vimentin IHC staining.

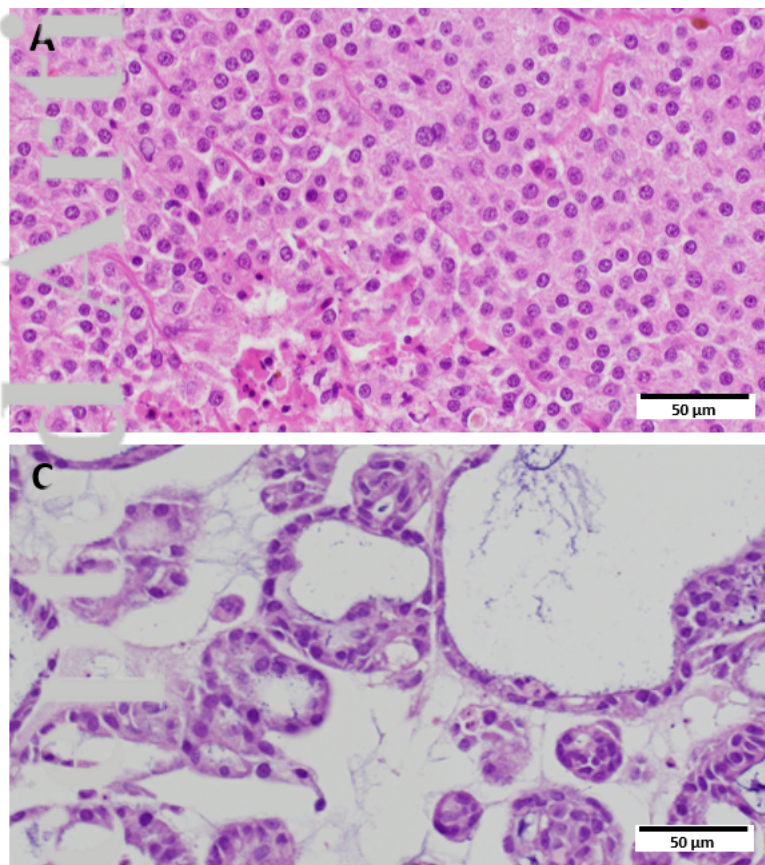
Figure 7: Plot of BAF for each SNP per chromosome (1-38, X): A. in healthy cells (EDTA-anticoagulated whole blood), B. in the cMTC N°2 primary tumor, C. in the cMTC N°2 organoid line.

Figure 8: Plot of LRR for each SNP per chromosome (1-38, X): A. in healthy cells (EDTA-anticoagulated whole blood), B. in the cMTC N°2 primary tumor, C. in the cMTC N°2 organoid line.





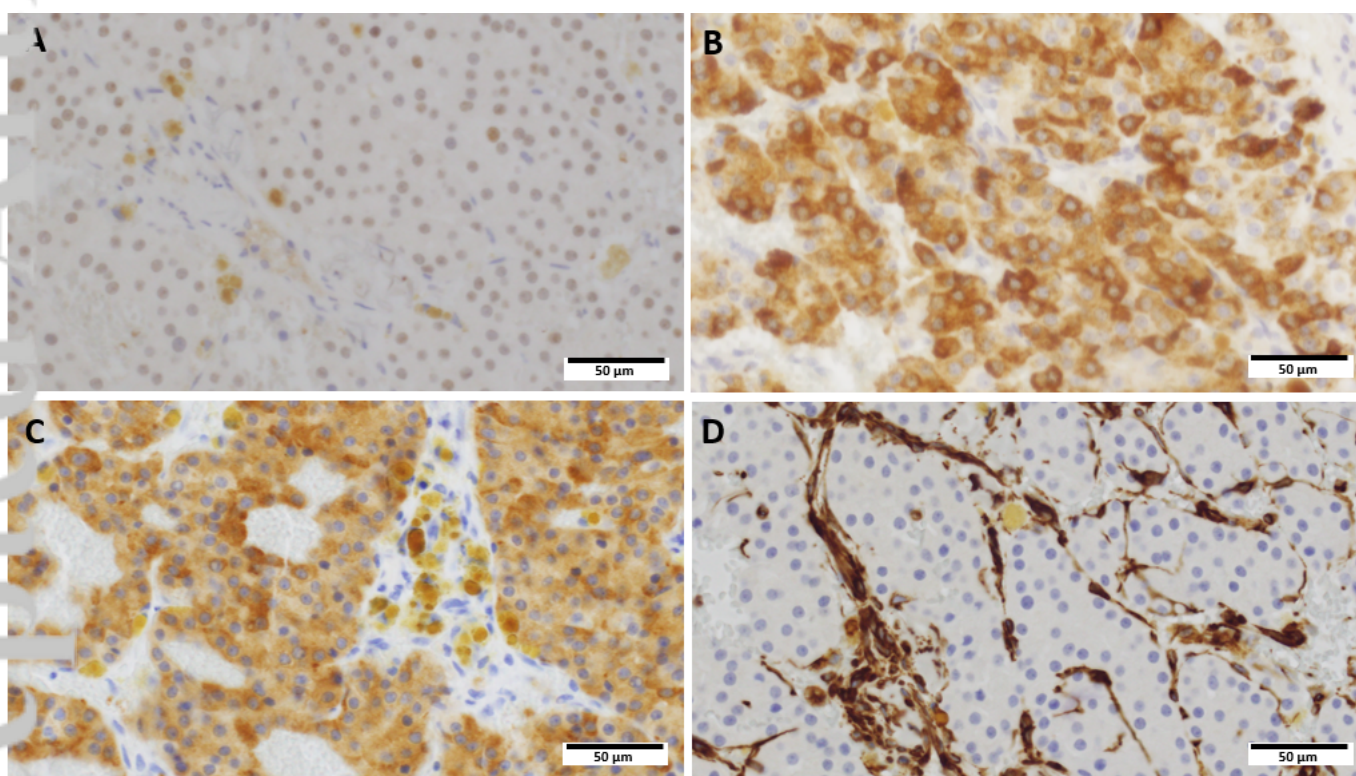
VCO\_12872\_Figure\_2.tif



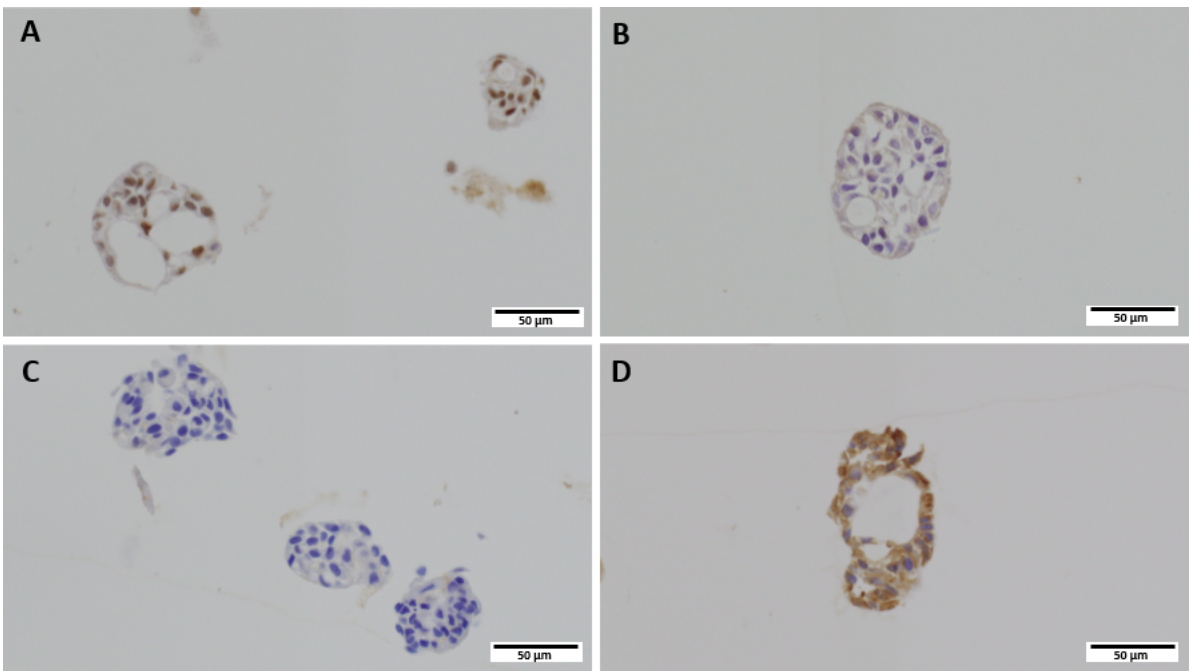
VCO\_12872\_Figure\_3.tif

Accepted Article

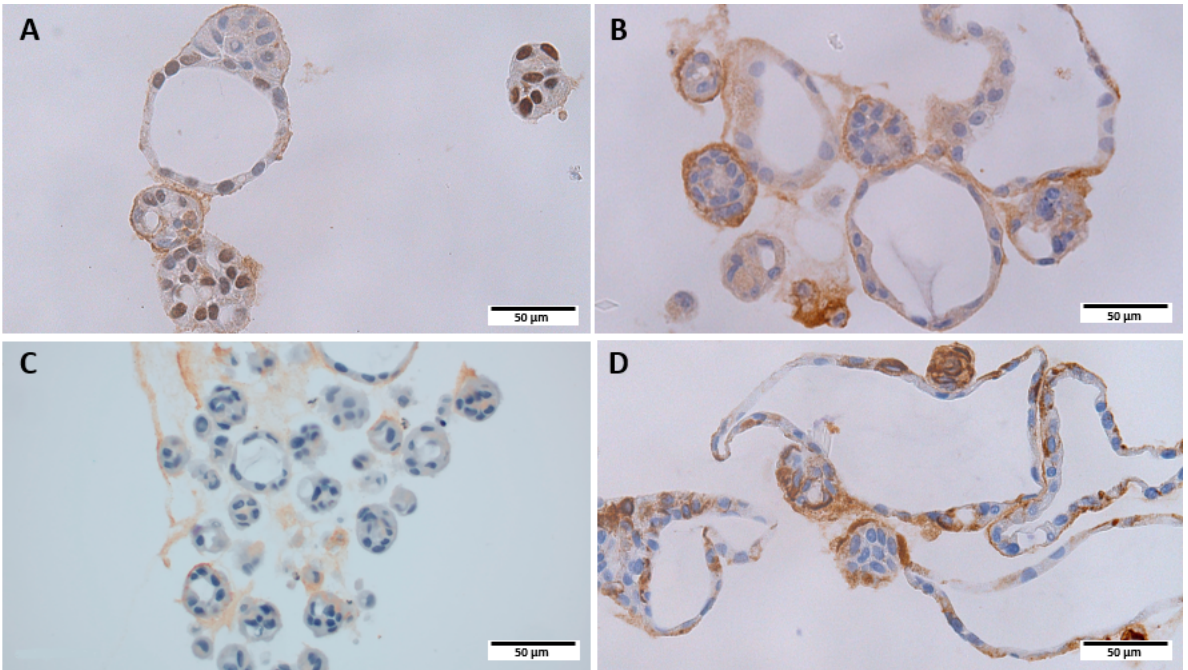




VCO\_12872\_Figure\_4.tif



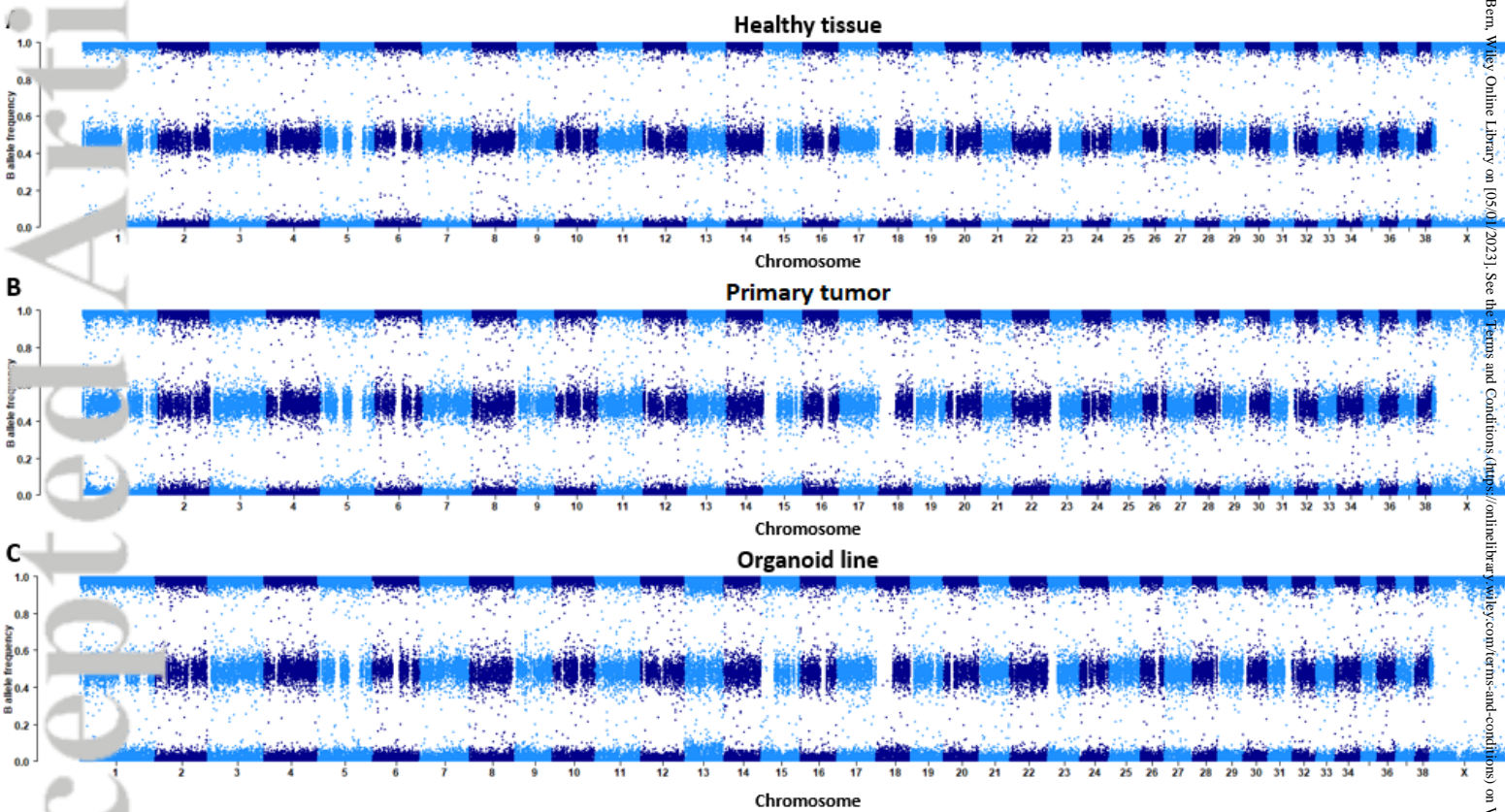
VCO\_12872\_Figure\_5.tif



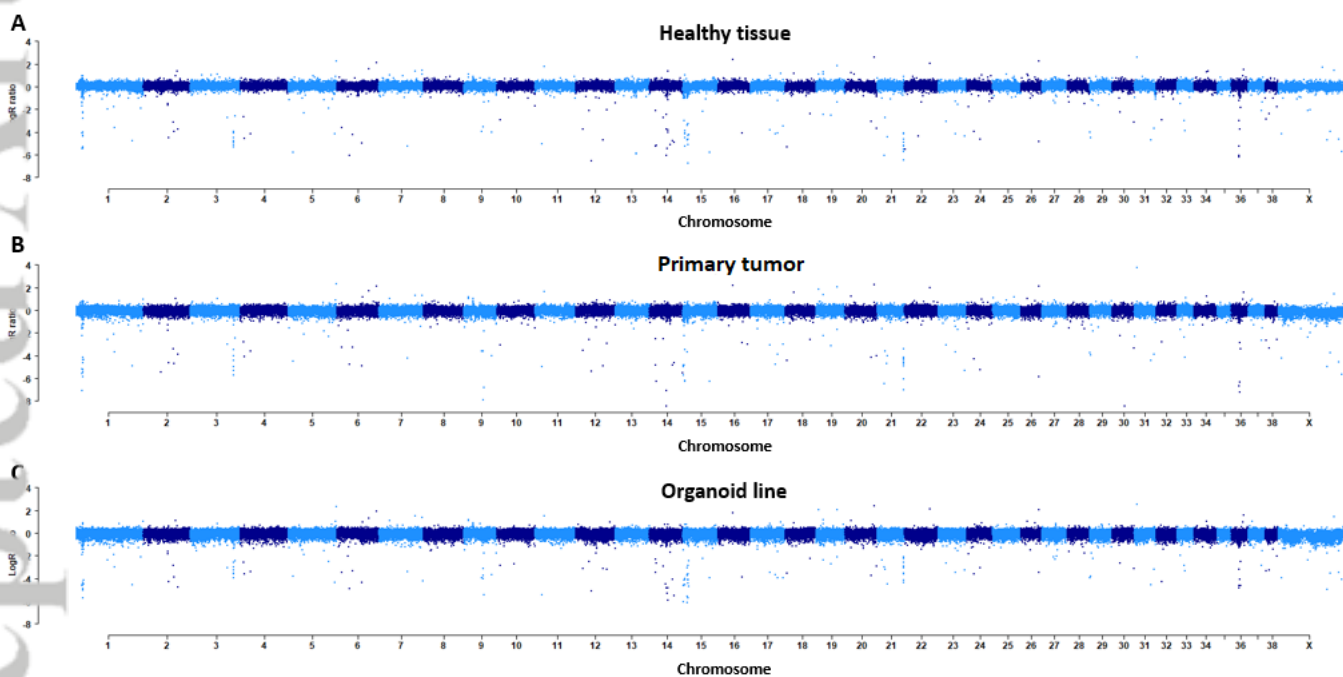
VCO\_12872\_Figure\_6.tif



Accepted Article



VCO\_12872\_Figure\_7.tif



VCO\_12872\_Figure\_8.tif

Table 1: Signalment, thyroid function status, TNM classification and tumor stage of the dogs with primary cMTC. Time in culture, highest passage number and reason to end culture of the cMTC cultures are also included.

cMTC N°	Primary cMTC tissue						cMTC culture		
	Breed	Age (years)	Sex	Thyroid function	TNM classification	Tumor stage	Time in culture (days)	Highest passage	Reason to end culture
1.	Mixed	10.5	MN	Euthyroid	T2aN0aM0	II	40	4	Bacterial contamination
2.	Beagle	10.5	M	Low TT4	T2aN1aM0	III	94	9	In culture until the end of the study
3.	Mixed	10	FN	Euthyroid	T2aN0aM0	II	33	2	No growth
4.	Mixed	8	F	Euthyroid	T3bN1aM0	III	32	2	No growth
5.	Podengo	12	MN	Hypothyroid	T2aN0aM0	II	8	1	No growth

Abbreviations: cMTC, canine medullary thyroid carcinoma; MN, male neutered; M, male; FN, female neutered; F, female; TT4, total thyroxine.

Table 1: Primary antibodies used for IHC.

Primary antibody	Antibody name	Antibody type	Dilution	Positive control tissue
TTF-1	Clone 8G7G3/1 <sup>a</sup>	Mouse monoclonal	1:50	Healthy canine thyroid gland
Thyroglobulin	A0251 <sup>b</sup>	Rabbit polyclonal	1:2000	Healthy canine thyroid gland
Calcitonin	A0576 <sup>b</sup>	Rabbit polyclonal	1:200	Healthy canine thyroid gland
Synaptophysin	Clone 27G12 <sup>c</sup>	Mouse monoclonal	1:200	Healthy canine adrenal gland
Vimentin	Clone V9 <sup>b</sup>	Mouse monoclonal	1:1000	Healthy canine parotid gland
Ki-67	Clone SP6 <sup>d</sup>	Rabbit monoclonal	1:50	High grade canine mast cell tumor
COX-2	Clone 33 <sup>e</sup>	Mouse monoclonal	1:20	Healthy canine kidney
P-glycoprotein	Clone C219 <sup>f</sup>	Mouse monoclonal	1:40	Healthy canine liver
VEGF	SPM225 <sup>g</sup>	Mouse monoclonal	1:20	Canine granulation tissue

Abbreviations: TTF-1, thyroid transcription factor-1; COX-2, cyclooxygenase-2; VEGF, vascular endothelial growth factor.

<sup>a</sup> Diagnostic BioSystems, Pleasanton, CA, USA

<sup>b</sup> Agilent, Santa Clara, Santa Clara, CA, USA

<sup>c</sup> Leica Biosystems, Wetzlar, Germany

<sup>d</sup> Cell Marque, Rocklin, CA, USA

<sup>e</sup> BD Biosciences, Franklin Lakes, NJ, USA

<sup>f</sup> BioLegend, San Diego, CA, USA

<sup>g</sup> Santa Cruz Biotechnology, Inc., Dallas, TX, USA

Table 3: Percentage of positive cells in primary cMTC N°2 tumor and derived organoids (P4, P8) for each primary antibody used for IHC.

	Primary tumor (%)	Organoids (P4, %)	Organoids (P8, %)
TTF-1	100	95	90 <sup>†</sup>
Thyroglobulin	0	0	0 <sup>†</sup>
Calcitonin	75	0	100 <sup>†</sup>
Synaptophysin	100	0	30 <sup>†</sup>
Vimentin	10	100	80 <sup>†</sup>
Ki-67 LI	2.37	56	10 <sup>†</sup>
COX-2	50	2	22.5 <sup>‡</sup>
P-glycoprotein	70	0	7.5 <sup>‡</sup>
VEGF	100	90	75 <sup>†</sup>

Abbreviations: P, passage; TTF-1, thyroid transcription factor-1; LI, labeling index; COX-2, cyclooxygenase-2; VEGF, vascular endothelial growth factor; NA, not available.

<sup>†</sup>, percentage of positive organoid cells in the control group of toceranib phosphate (0 nM) for the respective IHC antibody.

<sup>‡</sup>, mean percentage of positive cells in the control groups of meloxicam (0 μM) and toceranib phosphate (0 nM) for the respective IHC antibody.

Table 4: Percentage of positive cells in cMTC N°2 organoids (P8) incubated with different concentrations of meloxicam (0, 120 and 160  $\mu$ M) and TOC (0, 900 and 1200 nM) for COX-2, P-glycoprotein and VEGF.

	Organoids (P8)					
	Meloxicam			TOC		
	0 $\mu$ M	120 $\mu$ M	160 $\mu$ M	0 nM	900 nM	1200 nM
COX-2	30	20	20	15	NA	
P-glycoprotein	10	NA	0	5	NA	10
VEGF	NA			75	95	80

Abbreviations: P, passage; TOC, toceranib phosphate; COX-2, cyclooxygenase-2; VEGF, vascular endothelial growth factor; NA, not available.